Supplementary Materials

Supplementary Methods

HIF-1α knockdown or Inhibition

HIF-1α siRNAs were obtained from GenePharma (163971 and 163972, Suzhou China). The HIF-1α antibody was obtained from Abcam (51608, Cambridge, USA). The HIF-1α inhibitor 3-(5′-hydroxymethyl-2′-furyl)-1-benzylindazole (YC-1) was obtained from MedChem Express (Princeton, NJ, USA). Transfections were performed using Lipofectamine™ RNAiMAX Transfection Reagent (ThermoFisher, 13778150) according to the manufacturer's instructions. After 48 h of transfection, cells were then treated with the indicated exosomes and HUVECs were further analyzed for their tube-forming ability.

RNA sequencing and Bioinformatics

Sample collection and preparation

RNA quantification and qualification

RNA integrity was analyzed using the RNA Nano 6000 Assay Kit of the Bioanalyzer 2100 system (Agilent Technologies, CA, USA).

Library preparation

Total RNA was extracted using Trizol (ThermoFisher, USA, Cat no.: 710369) as input for the RNA isolation. Briefly, mRNA was purified from total RNA using poly-T oligo-conjugated magnetic beads. The enriched mRNAs were fragmented using divalent cations under elevated temperature in the First Strand Synthesis Reaction Buffer(5X). First strand cDNA was synthesized using random hexamer primers and

M-MuLV Reverse Transcriptase, followed by RNA degradation using RNaseH Second strand cDNA synthesis was subsequently performed using DNA Polymerase I and dNTPs. The remaining overhangs were converted into blunt ends via exonuclease/polymerase activities. After adenylation of 3' ends of DNA fragments, Adapters with hairpin loop structures were ligated to prepare for hybridization. In order to select cDNA fragments of preferentially 370~420 bp in length, the library fragments were purified using the AMPure XP system (Beckman Coulter, Beverly, USA). Then PCR was performed with Phusion High-Fidelity DNA polymerase, Universal PCR primers and Index (X) Primer. At last, PCR products were purified (AMPure XP system) and library quality was assessed on the Agilent Bioanalyzer 2100 system.

Clustering and sequencing

The clustering of the index-coded samples was performed on a cBot Cluster Generation System using TruSeq PE Cluster Kit v3-cBot-HS (Illumia) according to the manufacturer's instructions. Then library preparations were sequenced on an Illumina Novaseq platform and 150 bp paired-end reads were generated.

Data Analysis

Quality control

Raw data (raw reads) of fastq format were firstly processed to obtain clean data (clean reads) by removing reads containing adapter, reads containing N base and low quality reads. In this step, the Q20, Q30 and GC content the clean data were calculated. The clean data were used in downstream data analysis.

Reads mapping and Quantification

Reference genome (hg38) and gene model annotation files were downloaded directly from the genome website . Indexing and paired-end clean reads alignment was preformed using Hisat2 v2.0.5. FeatureCounts v1.5.0-p3 was used to count the reads numbers mapped to each transcripts, and the FPKM of each gene was calculated.

Differential expression analysis

Differential expression analysis of two conditions/groups (three biological replicates per condition) was performed using the DESeq2 R package (1.20.0). The P-values were adjusted using the Benjamini and Hochberg's approach for controlling the false discovery rate. Genes with adjusted P-values <0.05 found by DESeq2 were assigned as differentially expressed.

Enrichment analysis of differentially expressed genes

Gene Ontology (GO) enrichment analysis of differentially expressed genes was implemented by the clusterProfiler R package, in which gene length bias was corrected. GO terms with corrected P-value less than 0.05 were considered significantly enriched by differential expressed genes.

Supplementary Figures

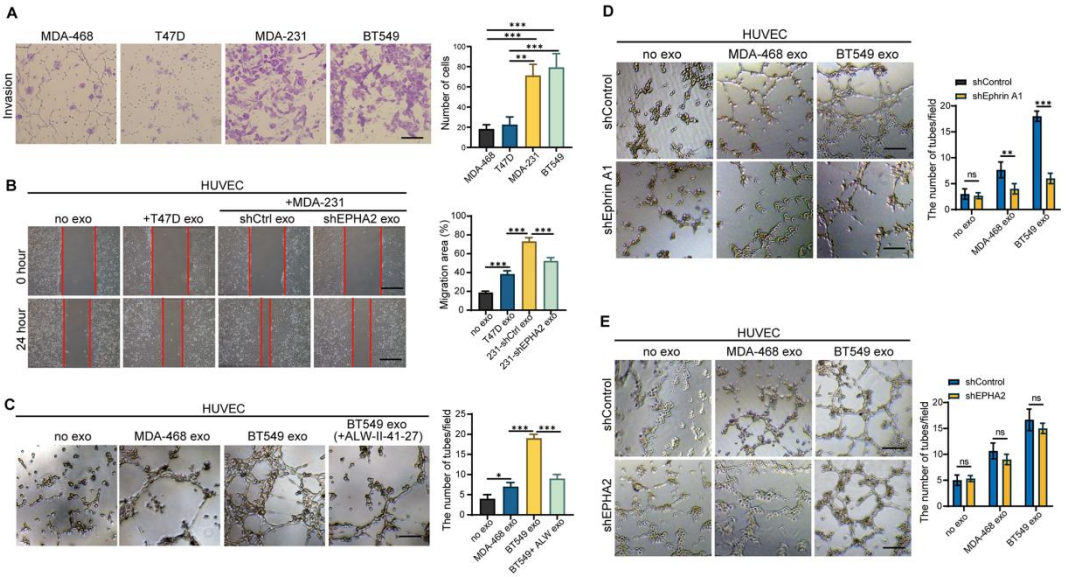

Figure S1

A The invasion ability of breast cancer cells with high metastatic potential (MDA-231 or BT-549) was significantly higher than that of breast cancer cells with low metastatic potential (MDA-468 or T47D). For cell invasion assay, 1×10^5 cells suspended in 200 μL of serum-free medium were loaded onto the upper chambers coated with Matrigel. The incubation time was 24 h. The statistical results were summarized in the right panel. **B** EPHA2-silenced HM-exos failed to promote the migration of endothelial cells. **C** The inhibitor-treated HM-Exos could not promote the tube formation of endothelial cells. **D** HM-Exos failed to promote the tube-forming ability of Ephrin A1-KD endothelial cells. **E** HM-Exos still promote the tube-forming ability of EPHA2-KD endothelial cells. Data were expressed as mean ± SD. All experiments were repeated at least three times. *P < 0.05, **P < 0.01, ***P < 0.001 and ns P > 0.05 indicate no statistical significance. Scale bar: 200 μm.

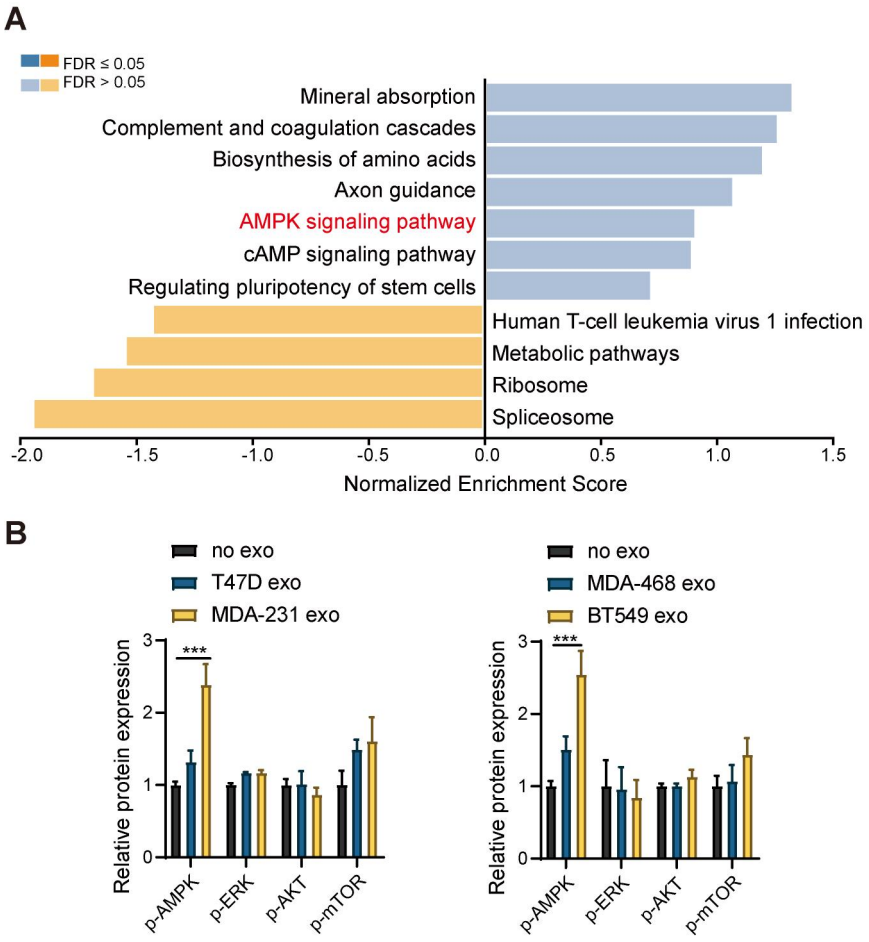

Figure S2

A Gene set enrichment analysis (GSEA) of the RNA-Seq data showed that the AMPK signaling pathway was induced in EPHA2-rich exosomes treated HUVECs compared with control exosome treated cells. FDR, False Discovery Rate. **B** Quantification of the western bloting images in Figure 5B. The analysis was performed using WB scans from three biological repeats.

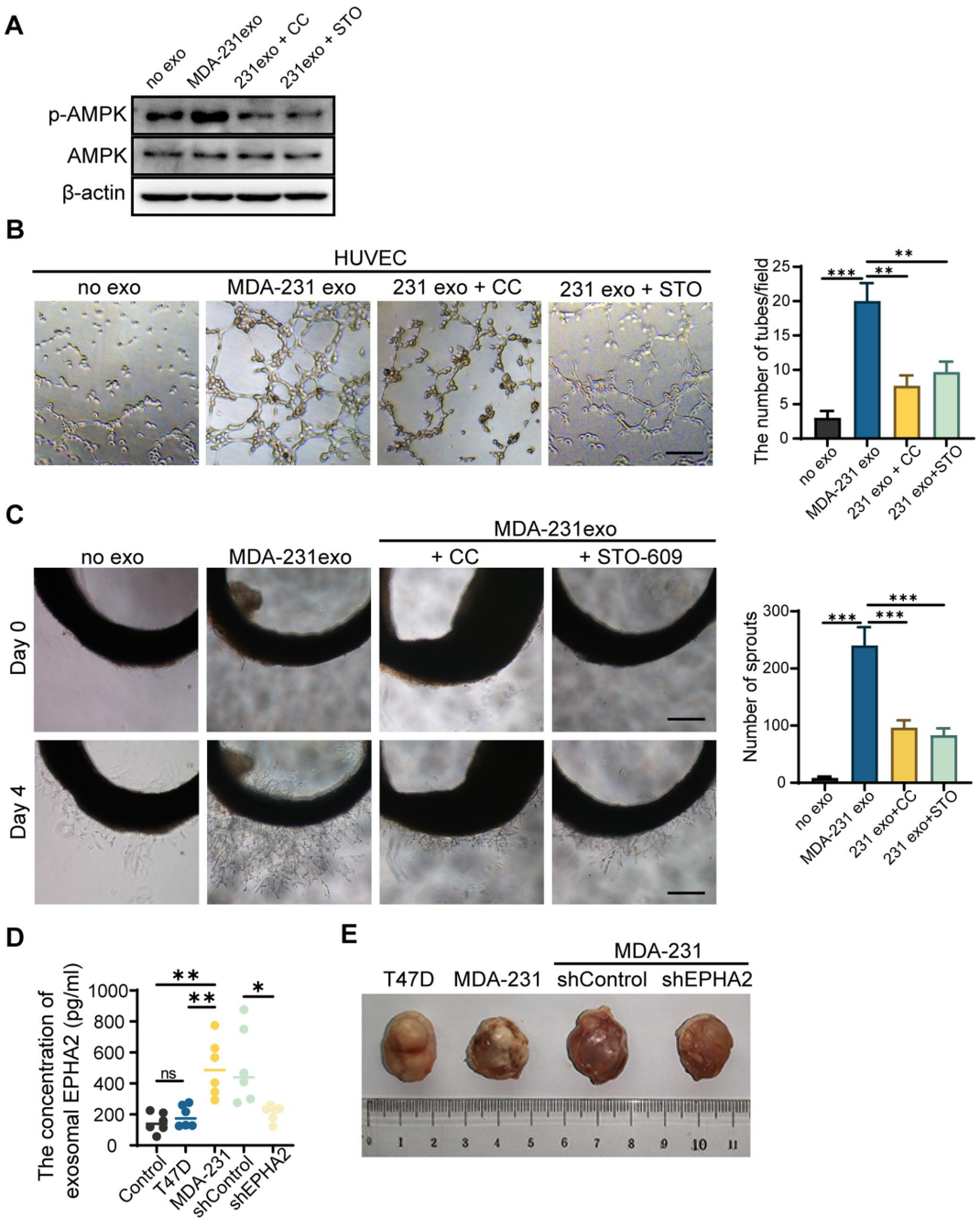

Figure S3

A Compound C or STO609 eliminated the phosphorylation of AMPK in HUVEC that incubated with HM-Exos. **B, C** Inhibition of AMPK signaling by Compound C or STO609 reduced the tube-forming and rat arterial ring outgrowth capacity in HM-Exos treated endothelial cells. **D** Exosomal EPHA2 was significantly upregulated in plasma of mice from the MDA-231 and MDA-231-shControl groups compared

with the T47D and MDA-231-shEPHA2 groups. **E** Representative images of subcutaneous tumor formed in mice. All experiments were repeated at least three times. *P < 0.05, **P < 0.01, ***P < 0.001 and ns P > 0.05 indicate no statistical significance. Scale bar: 200 μm.

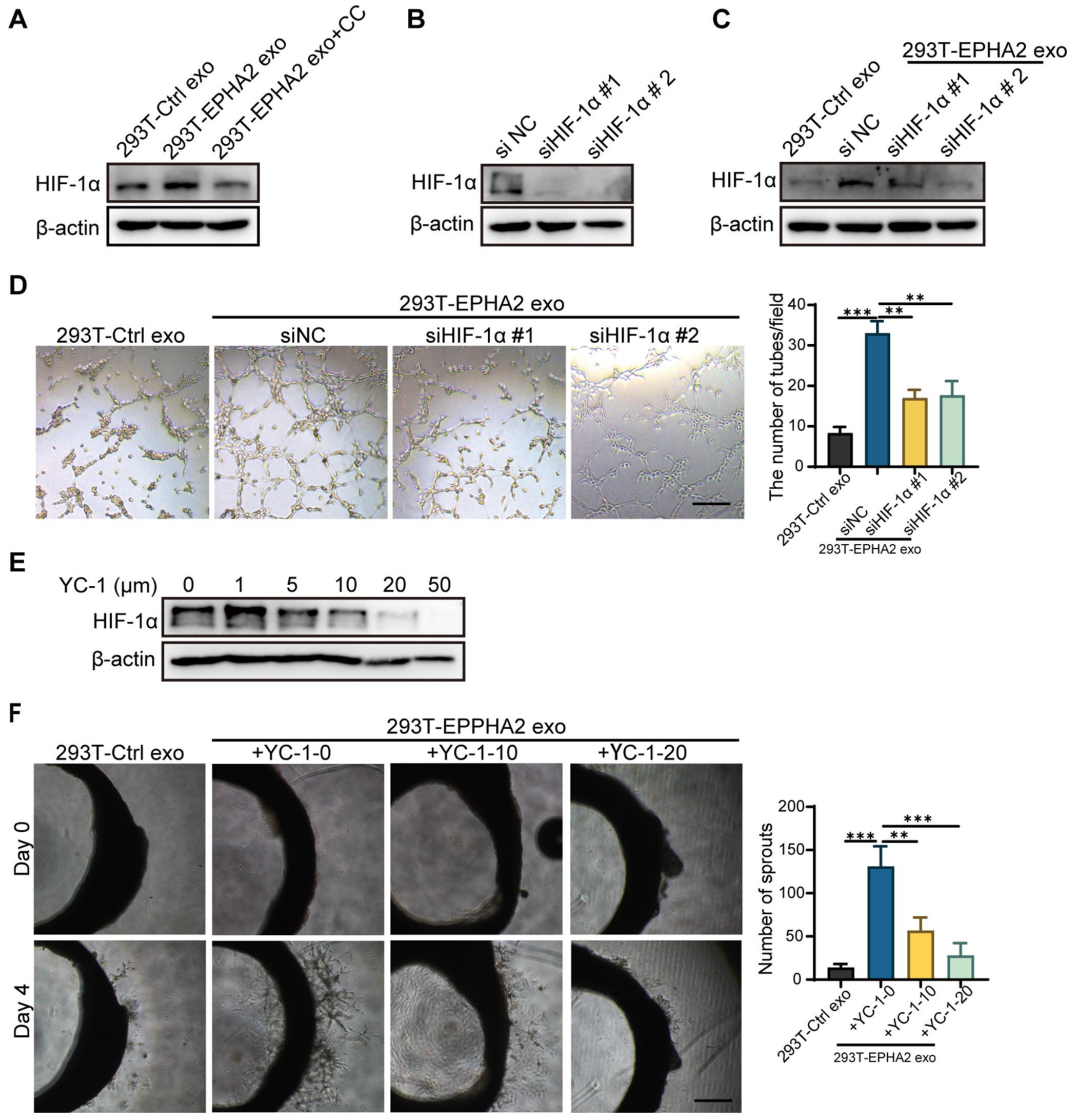

Figure S4

A EPHA2-rich exosomes increased HIF-1α protein levels in endothelial cells whereas Compound C inhibited the upregulation of HIF-1α by EPHA2-rich exosomes. **B** HIF-1α expression was silenced in endothelial cells. **C** EPHA2-rich exosomes failed to increase the HIF-1α protein levels in HIF-1α-KD cells. **D** EPHA2-rich exosomes failed to promote the tube-forming ability of HIF-1α-KD HUVECs. **E** YC-1 can inhibit the protein expression level of HIF-1α in endothelial cells. **F** YC-1 reduced the ability of microvessel growth in EPHA2-rich exosome-treated rat arterial rings.

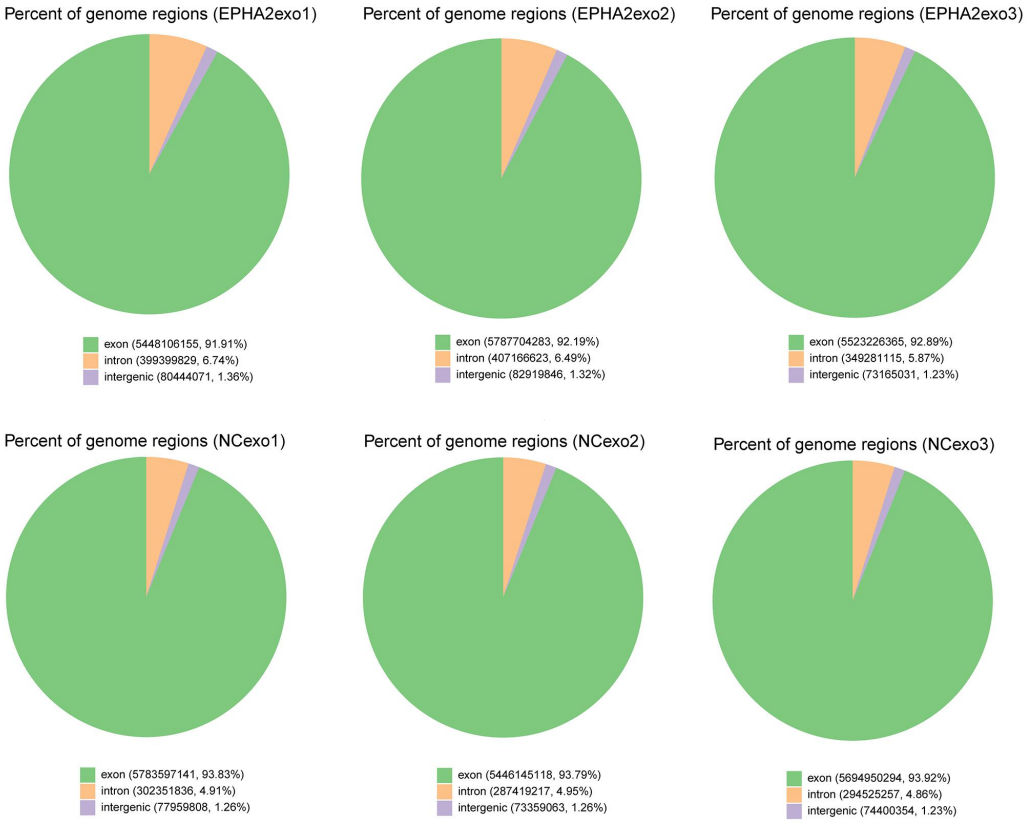

Figure S5 The percentage of reads that mapped to the mRNA

The percentage of reads that mapped to the mRNA. The mapping information of each technical replicate was shown as pie plot.

Supplementary Tables

Table S1. The shRNA sequences used in this study

Name	Sequence
shEPHA2 #1	5′-CTATTCTGTCAGTGTTAAA-3′
shEPHA2 #2	5′-GATAAGTTTCTATTCTGTCAG-3′
shEphrin-A1 #1	5′-AGAGGTGCGG GTTCTACATAG-3′
shEphrin-A1 #2	5′-GTCTTCTGGAACAGTTCAAAT-3′

Table S2. Primers used in this study

Name	Primers
mCherry-F	ACCTCCATAGAAGATTCTAGAGCCACCATGGTGAGCAAGGGCGAGGA
mCherry-R	TTCGAATTCGCTAGCTCTAGATTACTTGTACAGCTCGTCCATGCC
EPHA2-F	ACCTCCATAGAAGATTCTAGAGCCACCATGGAGCTCCAGG
EPHA2-R	TTCGAATTCGCTAGCTCTAGATTACTTGTACAGCTCGTCCATGCC
EPHA2-ΔRBD-F	ACCTCCATAGAAGATTCTAGAGCCACCATGGGCCTGGC
EPHA2-ΔRBD-R	TTCGAATTCGCTAGCTCTAGATTACTTGTACAGCTCGTCCATGCC
EPHA2-S897A-F	ACCTCCATAGAAGATTCTAGAGCCACCATGGAGCTCCAGG
EPHA2-S897A-R	TTCGAATTCGCTAGCTCTAGACTTACTTGTACAGCTCGTCCATGCC
EPHA2-D739N-F1	ACCTCCATAGAAGATTCTAGAGCCACCATGGAGCTCCAGG
EPHA2-D739N-R1	GGCAGCCAGATTACGGTGCACATAGTTCATGTTGGCC
EPHA2-D739N-F2	GTGCACCGTAATCTGGCTGCCCGCAACATCCTCGTCAA
EPHA2-D739N-R2	TTCGAATTCGCTAGCTCTAGACTTACTTGTACAGCTCGTCCATGCC
EPHA2-D739N-F3	CTCCCCAGCACGAGCGGCTCGGAGGGGGTGCCCTTCCGCAC
EPHA2-D739N-R3	AGCCGCTCGTGCTGGGGAGCCGGATAGACACGC

Table S3. Summary of RNA-Seq data quality

Sample	Raw reads	Clean reads	Clean bases	Error rate	Q20	GC %
EphA2exo1	45324432	42280544	6.34G	0.03	97.59	49.37
EphA2exo2	45356986	44599476	6.69G	0.03	97.85	48.95
EphA2exo3	45116568	42306052	6.35G	0.03	97.5	49.46
NCexo1	45727976	44177416	6.63G	0.03	97.72	50.57
NCexo2	43439160	41605440	6.24G	0.03	97.44	50.4
NCexo3	46196778	43249020	6.49G	0.03	97.51	50.31

Table S4. Statistics of comparisons between samples and reference genome

Exported data											
sample	**total reads**	**total_map**	**unique_map**	**multi_map**	**read1_map**	**read2_map**	**positive_map**	**negative_map**	**splice_map**	**unsplice_map**	**proper_map**
Eph	422	396179	384543	11636	192592	191950	192068	192475	176254	208288	373046
A2e	805	91(93.7	50(90.9	41(2.7	93(45.5	57(45.4	18(45.4	32(45.5	55(41.6	95(49.2	46(88.2
xo1	44	%)	5%)	5%)	5%)	%)	3%)	2%)	9%)	6%)	3%)
Eph	445	419291	407167	12123	204404	202762	203415	203752	185711	221455	397705
A2e	994	06(94.0	34(91.2	72(2.7	95(45.8	39(45.4	04(45.6	30(45.6	38(41.6	96(49.6	16(89.1
xo2	76	1%)	9%)	2%)	3%)	6%)	1%)	8%)	4%)	5%)	7%)
Eph	423	397322	385796	11525	193295	192501	192721	193075	182136	203660	374649
A2e	060	87(93.9	94(91.1	93(2.7	88(45.6	06(45.5	14(45.5	80(45.6	13(43.0	81(48.1	70(88.5
xo3	52	2%)	9%)	2%)	9%)	%)	5%)	4%)	5%)	4%)	6%)
	441	411878	400588	11290	200917	199670	200102	200485	188159	212428	390010
NCe	774	63(93.2	22(90.6	41(2.5	87(45.4	35(45.2	91(45.3	31(45.3	70(42.5	52(48.0	04(88.2
xo1	16	3%)	8%)	6%)	8%)	%)	%)	8%)	9%)	9%)	8%)
	416	387968	377383	10585	189223	188160	188498	188885	177835	199548	367153
NCe	054	98(93.2	65(90.7	33(2.5	35(45.4	30(45.2	61(45.3	04(45.4	13(42.7	52(47.9	88(88.2
xo2	40	5%)	1%)	4%)	8%)	2%)	1%)	%)	4%)	6%)	5%)
	432	405239	393721	11517	197188	196532	196670	197051	187323	206397	382356
NCe	490	61(93.7	62(91.0	99(2.6	81(45.5	81(45.4	03(45.4	59(45.5	94(43.3	68(47.7	66(88.4
xo3	20	%)	4%)	6%)	9%)	4%)	7%)	6%)	1%)	2%)	1%)